Proc. Nat. Acad. Sci. USA
Vol. 72, No. 7, pp. 2691–2695, July 1975
Cell Biology

Chromatin architecture: Investigation of a subunit of chromatin by dark field electron microscopy

(nucleohistone/DNA configuration/histone association/histone 1 depletion/electron scattering)

JOHN P. LANGMORE* AND JOHN C. WOOLEY

Department of Biophysics and *Enrico Fermi Institute, The University of Chicago, Chicago, Illinois 60637

Communicated by Albert V. Crewe, April 7, 1975

ABSTRACT **Dark field scanning electron microscopy of unstained, unfixed samples of chromatin, histone-1-depleted chromatin, and nucleohistone has been used to identify an apparent subunit of chromatin, namely a disk-shaped structure we term the unit particle, which is probably about 135 Å wide and 50 Å thick in the hydrated state. The unit particles are found at rather uniform intervals along thin DNA-like fibers. Histone 1 depletion leads to a bimodal distribution of these spacings. Our observations suggest that the unit particle consists of a loop of nucleoprotein, perhaps around a histone core.**

After many attempts, with limited success, to describe the structure of the eukaryotic genetic material as a continuous structure, investigators are now turning their attention to models of a more discontinuous structure, involving subunits which might be "assembled" into chromatin. The existence of such subunits has been inferred from experiments showing that the nuclease digestion of chromatin gives a discrete pattern of polynucleotide products (1–4) and that specific complexes between various histone molecules can be formed in solutions of isolated histone and in chromatin (5–7). Unfortunately, x-ray diffraction patterns have not yielded any information about the existence or the possibilities for the internal structure of the subunit, or the manner in which the subunits associate.

The electron microscope would seem to be the ideal tool for studying chromatin, since it can be used to visualize both long and short range order and to observe individual components of a heterogeneous system, as chromatin seems to be. However, little agreement on the ultrastructure of chromatin has been achieved due to the varying appearance of the objects visualized by conventional electron microscopy, by which a range of chromatin filaments from 15 to 300 Å wide has been observed (8). The filaments have often exhibited "knobbiness" (9) and sometimes a particulate nature (10–14). Olins and Olins (13) used the results of their microscopy to first suggest chromatin subunits composed of equimolar amounts of each of the five histones. Among the still unanswered questions are: (*1*) to what extent is the appearance of chromatin particles dependent upon the effects of fixation and staining, and (*2*) what is the internal structure of the particles?

This article is a brief report of our studies of chromatin structure in very dilute solutions, including gently isolated calf thymus chromatin, both intact and depleted of the very lysine-rich histone, H1, and shear-solubilized nucleohistone. We have eliminated several sources of artifacts by observing unfixed, unstained specimens in the high-resolution scanning transmission electron microscope (15–17). On the basis of our results, we propose a simple model for the internal structure of the basic subunit of chromatin, and speculate how such subunits might form the filaments found by conventional electron microscopy.

Abbreviation: H1, histone 1 (very lysine-rich).

METHODS

Sample Preparation. Histone migration and proteolysis were minimized by using low ionic strength media and by including sodium bisulfite. Nuclei were prepared from calf thymus essentially following Allfrey *et al.* (18) with the inclusion of 10 mM sodium bisulfite, and purified through 2.4 M sucrose. Minimally sheared chromatin, in the gel state, was prepared by hypotonic shock of the purified nuclei (19). Chromatin was quantitatively depleted of H1 (as assayed by gel electrophoresis, Amberlite CG 50 chromatography, 5% perchloric acid solubility, and also a 0.6 M NaCl wash; see ref. 20) by DNA-cellulose chromatography in 1 mM $MgCl_2$, 1 mM $NaPO_4$, pH 7.0, conditions which minimize exchange of the remaining histones (compare ref. 21). Nucleohistone was prepared by shear-solubilization of chromatin in the absence of sodium bisulfite, followed by sedimentation through 1.7 M sucrose (20).

The chemical composition and stoichiometry of the samples were characterized using the procedures of Bonner *et al.* (20). Intact chromatin possessed a total histone/DNA weight ratio of 1.12 ± 0.04, an H1/DNA ratio of 0.29 ± 0.02, and a non-histone protein/DNA ratio of 0.55 ± 0.03. The histone/DNA ratio of H1-depleted chromatin was 0.83 ± 0.02; no non-histone proteins were found. The nucleohistone had a ratio of histone/DNA of 1.02 ± 0.02 and an H1/DNA ratio of 0.14 ± 0.02; no non-histone proteins were found.

All specimen solutions were "desalted" immediately before preparation, by exclusion on Sephadex G-100 equilibrated with 1 mM $NaPO_4$, pH 7.0. About 2 μl of this 30–50 μg/ml solution of chromatin were then placed on a 20–30 Å thick hydrophilic carbon film, blotted, and air dried.

Electron Microscopy. All specimens were examined at 30 keV in dark field using the high-resolution scanning transmission electron microscope developed in the laboratory of Dr. A. V. Crewe (15–17). Microscope operating conditions were as described before, except that we chose not to outgas the specimen by baking (17). The elastically and inelastically scattered electron signals were usually simultaneously stored in digital form directly on magnetic tape, using a 512 × 512 picture element format (16, 17). At low instrumental magnification each picture element represented 15.4 Å at the specimen; at high magnification each picture element represented 4.96 Å. The magnification was determined from

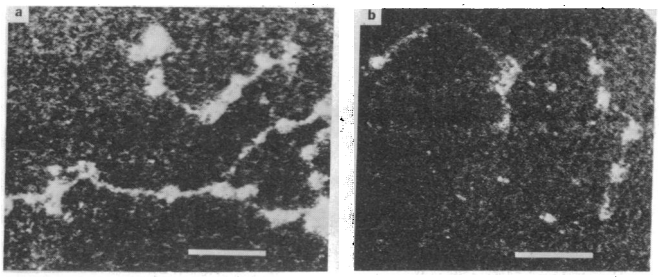

FIG. 1. Two typical high-dose, high-magnification elastic images of nucleohistone. The bars represent 500 Å. The specimen was not "desalted," but merely resuspended in 1 mM $NaPO_4$, leading to high atomic number solutes bound to the particles, but not the fibers.

a replica of a diffraction grating (2160 lines/mm) (16). The images were later replayed from magnetic tape onto film. To minimize radiation damage, we made low-magnification images at less than five incident electrons per $Å^2$. The contamination rate at low magnification was less than 1 Å/min.

Every particle in a micrograph was used for measurements, regardless of morphologic characteristics, provided it could be resolved from adjacent particles and was connected by thin fibers to two other particles. The center-to-center interparticle distances were measured along the contour of the fiber separating all particle pairs. All measurements were made to 0.1 mm accuracy on micrographs of 164,000× to 1,000,000× magnification. Both authors repeated measurements of the same particles, using prints of several magnifications and contrast ranges, to identify and remedy any systematic errors. The uncertainty assigned to any value is the standard deviation of the measurements.

RESULTS

The features of all of our specimens can be qualitatively described in terms of five structural classes.

Class 1 is the most extended form, and is characterized by long, uniform, unbranched fibers 20–30 Å wide and usually greater than 2000 Å long. Such fibers are likely to be single molecules of duplex DNA with little, if any, bound histone.

Class 2 is the most extended histone-bound form, characterized by unbranched fibers 20–30 Å in width and up to 5 μm or more in length, punctuated by circular particles, 90–150 Å wide. The particles are seldomly contiguous, and are not uniformly spaced.

Class 3 is more condensed than class 2, consisting of round particles 100–150 Å in width along a 20–50 Å wide fiber. It is distinguished from class 2 by *(a)* particles of more uniform size and shape, often possessing a distinct hole in the center, *(b)* fibers which are often 30–50 Å thick, which sometimes branch into two 20–30 Å wide fibers of equal width, and *(c)* smaller, more uniform spacings between particles.

Class 4 and class 5 consist of 120–350 Å wide filaments, and aggregates 300–10,000 Å in size, respectively. The small filaments usually exhibit a looping substructure, while the larger filaments appear more continuous.

In this paper we will concentrate on the class 2 and class 3 regions, since in the specimens described they constituted about 80% of the observed material.

Nucleohistone. Shear-solubilized nucleohistone was observed, since it has been extensively used in optical and x-ray scattering studies. In the microscope such preparations clearly show filaments of class 2 and class 3 structure, of alternating particle-fiber-particle configuration (Fig. 1). The average particle diameter was found on high magnification images to be 118 ± 7 Å. Many particles were either "U" shaped or circular with a hole in the center. The average interparticle spacing was 253 ± 75 Å (Fig. 2a). Two distinct types of interparticle fibers were discovered, those of 20–30 Å width, presumably containing a single duplex DNA molecule, and those of 30–50 Å width, often formed by the coalescence of two of the thinner fibers.

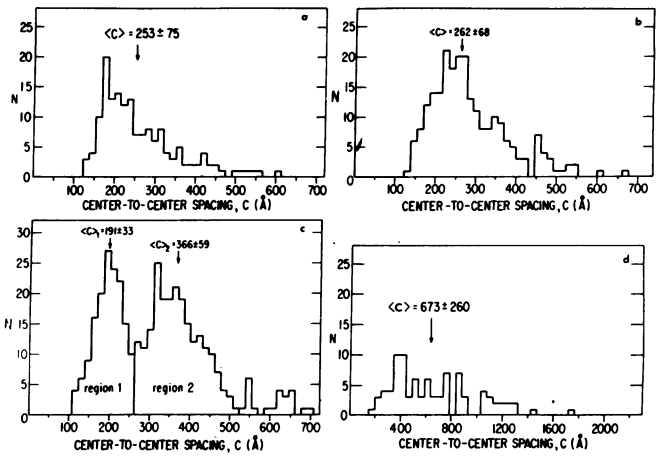

FIG. 2. Center-to-center interparticle spacing measurements, from (a) nucleohistone, (b) intact chromatin, (c) H1-depleted chromatin, and (d) extended, class 2, H1-depleted chromatin. The average spacing, ⟨C⟩, is determined from all spacings less than 450 Å in (a) and (b); from region 1 (100–260 Å) and region 2 (260–520 Å) in (c); from all spacings in (d).

Calf Thymus Chromatin. Because the nucleohistone preparation procedures involve extensive shearing and high salt conditions (which might lead to exchange or migration of the histone), we observed chromatin taken directly from a gel. These specimens possessed all five structural classes, with a predominance of class 3. The particle-fiber distinction is difficult to make in many areas, but is apparent from high-magnification images (Fig. 3). The interparticle spacing distribution (Fig. 2b) is similar to that found in nucleohistone, but the particle diameters are on the average larger (Fig. 4a). The average diameter of 150 Å was determined from low-magnification images. This is an overestimate, since these images have a resolution element of 15.4 Å, and thus cause the image to appear about 15 Å larger than the object. Measurements of images at high magnification give a more accurate estimate of the average diameter to be 134 Å.

By relating the scattered electron signals to the mass thickness within the particles we have found that even the particles without holes are flat disks (not spheres), often with a less massive center. Some of the particles exhibit a central hole or depression (Fig. 3b and c). However, caution is needed in interpreting these structures, since many may come from fortuitous looping of histone-bound DNA as a result of local unfolding of the structure. The hollow appearance of these unstained particles should be distinguished from the features often seen in images of stained or shadowed particles due to build-up of electron dense material around the margin of the object (compare ref. 22). We have determined the central hole diameters to be 36 ± 9 Å in particles of typical size (134 ± 14 Å).

The circular disk appearances of the particles suggest that the DNA is formed into an open loop (or loops) of 30–60 Å radius, within the particles. The appearance of a central hole could be the result, for example, of the relaxation of hydro-

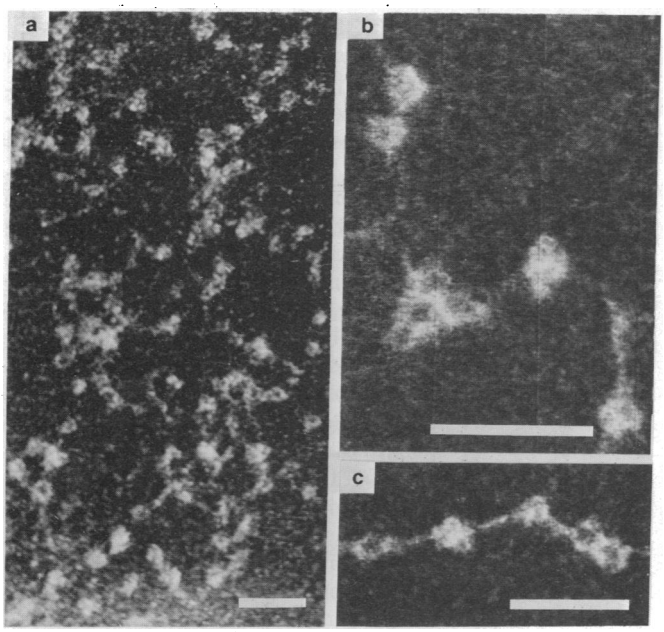

FIG. 3. Inelastic micrographs of chromatin, showing (a) particles, fibers, and loops of nucleoprotein at low magnification, and (b) and (c) particles and fibers of two areas at high magnification. The bars represent 500 Å.

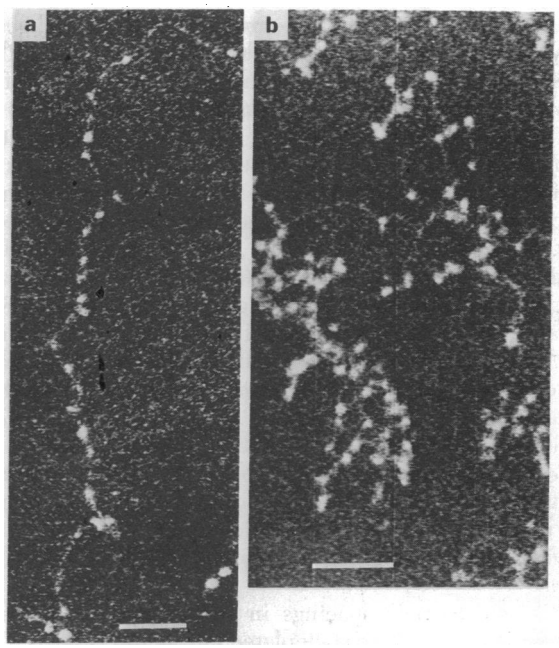

FIG. 5. Low-magnification inelastic images of H1-depleted chromatin in (a) a class 2 area, and (b) a class 3 area. The bars represent 1000 Å.

phobic histone–histone interactions at the center of the particles. Alternatively, both heavy core and light core particles could exist in solution, one being a different conformational or stoichiometric form of the other.

The average interparticle fiber diameter was 38 ± 12 Å. The large fiber widths and occasional branch points indicate that two DNA molecules were sometimes present.

H1-Depleted Calf Thymus Chromatin. Removal of H1 and the residual amounts of non-histone proteins by DNA-cellulose exchange reduces the amount of aggregation found, and leads to material dominated by class 2 and class 3 structures with small amounts of the others. The images of the particles (Fig. 5), and the distribution of particle widths (Fig. 4b) are very similar to those found in undepleted material. Again, since these data are taken at low magnification, a better estimate of the mean diameter is 131 Å. The ratio of the mean particle widths measured parallel to those perpendicular to the fiber is 1.0 ± 0.25, showing that even if some of the particles are asymmetrical, there is no preferred orientation with respect to the fiber. Often two 20–30 Å wide fibers are found between particles, and many of the particles have less intense centers.

The spatial distribution of mass in some of these particles is more clearly presented in Fig. 6. The scattered electron currents have been converted to a probability for inelastic scattering along six horizontal lines in the image. The height of the trace at each point is proportional to the mass thick-

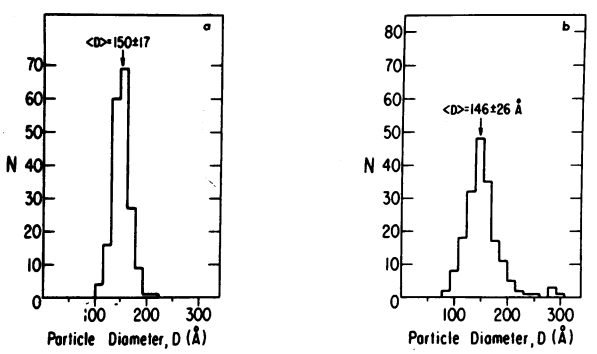

FIG. 4. Apparent particle diameters as measured at low magnification, from (a) intact chromatin, and (b) H1-depleted chromatin. The true particle diameters are about 15 Å smaller.

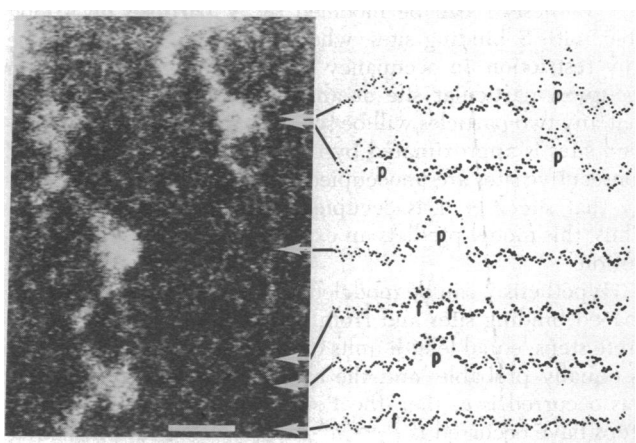

FIG. 6. A portion of a high-magnification image of H1-depleted chromatin. The bar represents 200 Å. The probability for inelastic scattering is presented on the right, along six horizontal lines in the image as indicated by arrows. The first two traces represent averages over two successive lines; the last four traces over five successive scan lines. Scans over particles and fibers are indicated by the letters p and f, respectively. A light core particle and twin interparticle fibers are presented. The case for the disk-shaped particles is strengthened by the observation that the mass thickness of some of the particles is no greater than that of the 40–50 Å wide fibers, while others of the same width have about twice the mass thickness of the thinner particles (and thus twice the mass), and perhaps represent two stacked disks. Oblong projections of objects having high mass thicknesses, such as that in the top center of the micrograph, might represent particles standing on end.

ness at that point on the specimen. The mass thickness is fairly constant across each particle, unlike that expected for a spherical particle. We can calculate the thickness, t, of the dehydrated specimen at every point with the equation $t = P_{IN}/(\bar{\sigma}_{IN}\rho_A F_M)$ (ref. 23), where P_{IN} is the experimentally determined probability for inelastic scattering, $\bar{\sigma}_{IN}$ is the specific cross section for inelastic scattering from chromatin (theoretically predicted and experimentally determined to be 0.003 ± 10% Å^2/dalton at 31 keV), ρ_A is the anhydrous density of the specimen, estimated to be the reciprocal of the specific volume (ρ_A = 1.47 g/cm^3, ref. 24), and F_M is the experimentally determined fraction of the initial mass which was *not* lost during irradiation of the specimen (in this case F_M = 0.55 ± 10%). This calculation gives a thickness of 35 ± 10 Å for these and similar particles. If we assume that the internal hydration of chromatin is 0.4 g of H_2O per g of chromatin [that found for the 30S ribosomal subunit of *Escherichia coli* (25)] and that air drying of particles results in a decrease in particle height, with no change in width (26), these particles are only 55 ± 20 Å thick in solution.

The interparticle spacings in the class 3 areas are the unique feature of the H1-depleted chromatin (Fig. 2c). Two separate regions exist, with modes at about 200 Å and at about 350 Å, containing 40% and 55% of the observed spacings, respectively. The bimodality is evident even in groups of particles in the same area of the specimen. The removal of H1 might promote the unfolding of 100–150 Å of fiber which would otherwise have been tightly bound to the particle.

It is interesting to determine whether the observed interparticle spacing distributions are consistent with only one of two simple hypotheses: *(1)* The particles are randomly distributed along the fiber, or *(2)* The particles are non-randomly distributed on the fiber.

Hypothesis 1 can be modeled by N particles on a long fiber with S binding sites, where $(N/S) = a \ll 1$, and the only restriction on occupancy is that only one particle can occupy a particular site at any time. The probability, P_z, that any two particles will be separated by exactly Z unoccupied sites is approximated by the Poisson probability that Z consecutive sites are unoccupied, multiplied by the probability that site Z + 1 is occupied, namely $P_z = \exp(-Za)a$. Thus, this model predicts an exponentially decreasing distribution.

Hypothesis 2 can be modeled by particles fixed to equally spaced binding sites and from which can be drawn, in discrete steps, equal length units of fiber. If each extension step is equally probable, and the average number of steps that has occurred is a, then the Poisson probability that Z such steps have occurred is $P_Z = a^Z \exp(-a)/Z!$. Using this equation we can generate a spacing distribution similar to those we find experimentally.

The data presented in Fig. 2 are clearly consistent with hypothesis 2, but not with hypothesis 1. A wide range of fixed-particle models would be consistent with the data, but the facts that the most probable fiber length is not close to zero, and that the observed distributions can be bimodal and do not decrease exponentially even in highly extended chromatin (Fig. 2d) show that the particles are not randomly distributed. We conclude that a mechanism must exist for regulating the distance between particles and that this mechanism has not been disrupted by our preparative techniques. In addition, the data suggest that the particles cannot migrate along the fiber.

DISCUSSION

Visualization in dark field by the scanning transmission electron microscope of unstained calf thymus chromatin, isolated under conditions minimizing proteolysis and histone migration, has yielded convincing evidence for periodically alternating condensed regions, or particles, and extended regions, or fibers, along the chromatin filament. In brief, we conclude the following about the architecture of chromatin: *(1)* The chromatin filaments in non-aggregated regions consist of particles 134 ± 14 Å in diameter, spaced 262 ± 68 Å apart along a 20–50 Å wide fiber involving one and often two DNA molecules. *(2)* The particles are probably not spherical but disk-shaped, being about 50 Å thick when hydrated, and sometimes have a central hole 36 ± 9 Å in diameter. *(3)* The particle size, height, circular shape, and lack of orientation with respect to the filament axis are most consistent with the hypothesis that the "backbone" to the structure is a loop (or loops) of DNA with a radius of 30–60 Å, held in place by a very stable histone superstructure. *(4)* Depletion of H1 by the DNA-cellulose method does not seriously alter the features of the particles or fibers, although a unique bimodal center-to-center spacing is produced. *(5)* The particles are not randomly distributed along the fiber.

The validity of these conclusions is supported by independent evidence. Air drying of hydrated molecules such as ribosomes and viruses seems to cause a reduction in height but not a change in width (26, 27). By our techniques we find the apparent width of tobacco mosaic virus particles and the dimensions of the ribosomal subunits from *E. coli* to be consistent with the x-ray data on the volumes of hydrated samples (23). The accuracy of our thickness determinations has been tested by height or molecular weight determination of ribosomal subunits, tobacco mosaic virus, and micrococcal-nuclease resistant chromatin fragments, "*PS*-particles" (1). In the studies reported here, salt artifacts are unlikely, since analysis of the ratio of elastic to inelastic scattering (17) indicates that none of the chromatin phases contain more than two bound salt molecules per DNA base. It should be noted that increasing the ionic strength causes serious artifacts. In addition, electron radiation damage to our chromatin samples does not significantly change the morphologic features observed over an exposure range from 0.15 to 1000 electrons/Å^2.

It should be pointed out that many of the conventional staining or shadowing techniques have not been shown to yield reliable results, especially for highly hydrated structures. For example, *(a)* negative staining, positive staining, or shadowing of ribosomal subunits yields incorrect particle volumes (25), *(b)* stain structure changes rapidly in the electron beams (28, 29), *(c)* negative stains seem to penetrate many structures and cause local distortions of dimensions (30), and *(d)* staining causes clumping of particles, such as polysomes, making distance measurements unreliable (31). In addition, salt artifacts cannot be identified in conventional studies. Of particular relevance to interpreting previous electron microscopic images of chromatin are the changes in sedimentation velocity resulting from even mild formaldehyde fixation of nucleohistone (32), and the likelihood of a strong interaction between phosphotungstic acid and the basic residues of histones, as well as between uranyl salts and the DNA.

The differences in specimen preparation and observation techniques may lead to the difficulty in reconciling our results with those regarding "ν bodies," which have been reported to be 70 Å spheres with greater than 300,000 molecu-

lar weight (13). We suggest, however, that the 2.8 g/cm^3 density required for such particles is inconsistent with that known for any biological molecule. To eliminate any confusion between what may not be identical structures, we propose the name unit particle for the chromatin subunits we observe. Particles similar in size (100–200 Å) to the unit particles were observed by Slayter *et al.* (10).

Unit particles provide a more tenable basis for extensive histone–histone interactions than do spherical particles. Histone–histone interactions between disks could lead to lateral assembly and possible compaction into the 100–150 Å and 200–300 Å thick filaments found in thin-section microscopy.

The concept of a loop of DNA, probably around a histone core, alternating with a more extended segment of DNA, places strict constraints upon the structural models to be considered. We will discuss the implications of our results in detail elsewhere, but four features should be pointed out here. *(1)* In dilute solutions of nucleohistone, an x-ray pattern due only to the particles and the fibers, and not to their packing, might be found. The radius of gyration we calculate for toroids or homogeneous disks of the size of our unit particles is about 50 Å, roughly corresponding to the experimental radius of gyration in dilute solutions (33). *(2)* If a nucleohistone gel were to be oriented by hydrodynamic shearing, the planes of the disks and the axis of the fibers would orient along the shear direction, leading to a net orientation of the DNA molecular axis, resulting in the meridional orientation of the x-ray pattern (34) and absorption dichroic ratios greater than one (35). However, lateral stacking of the particles in the oriented gels might lead to equatorial orientation of the 55 Å reflection. *(3)* The interparticle spacings might provide the basis for the recent observations by neutron diffraction of 400 and 200 Å spacings which seem to be concentration independent (36). *(4)* The significant amount of free fiber(s) which can be associated with the unit particles might provide binding sites for non-histone proteins without requiring extensive restructuring of the histone-histone, histone–DNA or particle–particle interactions.

It is hoped that our concept of the structure of the unit particle will stimulate further experiments to determine the internal organization of the unit and the role it plays in the architecture of the thick filaments of chromatin.

Note Added in Proof. Recent examination of intact calf thymus chromatin which had been extensively fixed with formaldehyde in either 0.5 mM $NaPO_4$, 0.15 M KCl, or 0.65 M NaCl has confirmed the existence of unit particles over this wide range of ionic conditions, and that fixation does not seem to change the size or morphologic features of the particles. Furthermore, silicotungstic acid has been found to positively stain the histones within particles, but not bind to the interparticle fibers, suggesting that reactive histone groups are not present in the fibers, and that similar tungstates might not be reliable negative stains for chromatin.

We wish to acknowledge the encouragement and support of R. B. Uretz and A. V. Crewe. This work was supported by U.S. Public Health Service CA2739 and the Energy Research and Development Administration.

1. Rill, R. & Van Holde, K. E. (1973) *J. Biol. Chem.* **248**, 1080–1083.
2. Hewish, D. R. & Burgoyne, L. A. (1973) *Biochem. Biophys. Res. Commun.* **52**, 504–510.
3. Clark, R. J. & Felsenfeld, G. (1974) *Biochemistry* **13**, 3622–3628.
4. Noll, M. (1974) *Nature* **251**, 249–251.
5. D'Anna, J. A. & Isenberg, I. (1974) *Biochemistry* **13**, 2098–2104.
6. Kornberg, R. D. & Thomas, J. O. (1974) *Science* **184**, 865–868.
7. Martinson, H. G. & McCarthy, B. J. (1975) *Biochemistry* **14**, 1073–1078.
8. Comings, D. E. (1972) in *Advances in Human Genetics*, eds. Harris, H. & Hirschhorn, K. (Plenum Press, New York), Vol. 3, pp. 237–431.
9. Ris, H. & Kubai, D. F. (1970) *Annu. Rev. Genet.* **4**, 263–294.
10. Slayter, H. S., Shih, T. Y., Adler, A. J. & Fasman, G. D. (1972) *Biochemistry* **11**, 3044–3054.
11. Olins, A. L. & Olins, D. E. (1973) *J. Cell Biol.* **59**, 252a.
12. Woodcock, C. L. F. (1973) *J. Cell Biol.* **59**, 368a.
13. Olins, A. L. & Olins, D. E. (1974) *Science* **183**, 330–331.
14. Langmore, J. P. & Wooley, J. C. (1974) *J. Cell Biol.* **63**, 185a.
15. Crewe, A. V. & Wall, J. (1970) *J. Mol. Biol.* **48**, 375–393.
16. Wall, J., Langmore, J. P., Isaacson, M. & Crewe, A. V. (1974) *Proc. Nat. Acad. Sci. USA* **71**, 1–5.
17. Isaacson, M., Langmore, J. P. & Wall, J. (1974) in *Scanning Electron Microscopy/1974*, ed. Johari, O. (IIT Research Institute, Chicago, Ill.), pp. 19–26.
18. Allfrey, V. G., Littau, V. C. & Mirsky, A. E. (1964) *J. Cell Biol.* **21**, 213–231.
19. Panyim, S. & Chalkley, R. (1969) *Biochemistry* **8**, 3972–3979.
20. Bonner, J., Chalkley, G. R., Dahmus, M., Fambrough, D., Fujimura, F., Huang, R. C., Huberman, J., Jansen, R., Marushige, K., Ohlenbush, H., Olivera, B. & Widholm, J. (1968) in *Methods in Enzymology*, eds. Grossman, L. & Moldave, K. (Academic Press, New York), Vol. 12B, pp. 3–64.
21. Ilyin, Y., Varshavsky, A., Mickelsaar, J. & Georgiev, G. (1971) *Eur. J. Biochem.* **22**, 235–245.
22. Slayter, E. M. (1969) in *Physical Principles and Techniques of Protein Chemistry*, ed. Leach, S. J. (Academic Press, New York), Part A, pp. 2–58.
23. Langmore, J. P. (1975) Ph.D. Dissertation, University of Chicago.
24. Zubay, G. & Doty, P. (1959) *J. Mol. Biol.* **1**, 1–20.
25. Van Holde, K. E. & Hill, W. E. (1974) in *Ribosomes*, eds. Nomura, M., Tissieres, A. & Lengyel, P. (Cold Spring Harbor Laboratory, Cold Spring Harbor, N.Y.), pp. 53–91.
26. Hart, R. G. (1962) *Biochim. Biophys. Acta* **60**, 629–637.
27. Henkelman, R. M. (1973) Ph.D. Dissertation, University of Toronto.
28. Williams, R. C. & Fisher, H. W. (1970) *J. Mol. Biol.* **52**, 121–123.
29. Unwin, P. N. T. (1974) *J. Mol. Biol.* **87**, 657–670
30. Klug, A. & Finch, J. T. (1965) *J. Mol. Biol.* **11**, 403–423.
31. Slayter, H. S., Warner, J. R., Rich, A. & Hall, C. E. (1963) *J. Mol. Biol.* **7**, 652–657
32. Brutlag, D., Schlehuber, C. & Bonner, J. (1969) *Biochemistry* **8**, 3214–3218.
33. Bram, S. & Ris, H. (1971) *J. Mol. Biol.* **55**, 325–336.
34. Pardon, J. F., Richards, B. M. & Cotter, R. I. (1973) *Cold Spring Harbor Symp. Quant. Biol.* **38**, 75–86.
35. Wooley, J. C. & Uretz, R. B. (1974) *J. Cell Biol.* **63**, 378a.
36. Bram, S., Butler-Browne, G., Baudy, P. & Ibel, K. (1975) *Proc. Nat. Acad. Sci. USA* **72**, 1043–1045.